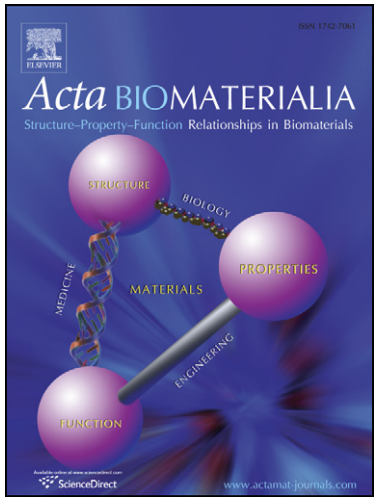

Base-metal dental casting alloy biocompatibility assessment using a human-derived 3D oral mucosal model

E.L. McGinley, G.P. Moran, G.J.P. Fleming

PII: S1742-7061(11)00370-9
DOI: 10.1016/j.actbio.2011.08.017
Reference: ACTBIO 1887

To appear in: *Acta Biomaterialia*

Received Date: 8 June 2011
Revised Date: 15 August 2011
Accepted Date: 17 August 2011

Please cite this article as: McGinley, E.L., Moran, G.P., Fleming, G.J.P., Base-metal dental casting alloy biocompatibility assessment using a human-derived 3D oral mucosal model, *Acta Biomaterialia* (2011), doi: 10.1016/j.actbio.2011.08.017

Base-metal dental casting alloy biocompatibility assessment using a human-derived 3D oral mucosal model

McGinley, E.L[1], Moran, G.P.[2] and Fleming G.J.P.[1]

[1]Materials Science Unit, Division of Oral Biosciences, Dublin Dental University Hospital, Trinity College Dublin, Ireland.

[2]Microbiology Research Unit, Division of Oral Biosciences, Dublin Dental University Hospital, Trinity College Dublin, Ireland.

Keywords: Biocompatibility, Dental casting alloys, Inflammation, Oxidative stress, ICP-MS.

Running title: Dental alloy biocompatibility using 3D oral mucosal models

Corresponding Author: Emma Louise McGinley,
Materials Science Unit,
Division of Oral Biosciences,
Dublin Dental University Hospital,
Trinity College Dublin,
Dublin,
Ireland.

Telephone: 00 353 1 612 7371

Fax: 00 353 1 612 7297

email emmalouise.mcginley@dental.tcd.ie

Abstract

Nickel-chromium (Ni-Cr) alloys used in fixed prosthodontics have been associated with type IV nickel-induced hypersensitivity. We hypothesized the full-thickness human-derived oral mucosa model employed for biocompatibility testing of **base-metal** dental alloy**s** would provide insights into mechanisms of nickel-induced toxicity. Primary oral keratinocytes and gingival fibroblasts were seeded onto Alloderm™ and maintained until full-thickness was achieved prior to Ni-Cr and cobalt-chromium (Co-Cr) alloy-disc exposure (2-72 h). Biocompatibility assessment involved histological analyses with cell viability measurements, oxidative stress responses, inflammatory cytokine expression and cellular toxicity analyses. Inductively coupled plasma mass spectrometry (ICP-MS) analysis determined elemental ion release levels. We detected adverse morphology with significant reductions in cell viability, significant increases in oxidative stress, inflammatory cytokine expression and cellular toxicity for the Ni-Cr alloy-treated oral mucosal models compared with untreated oral mucosal models and adverse effects were increased for the Ni-Cr alloy that leached the most nickel. Co-Cr demonstrated significantly enhanced biocompatibility compared with Ni-Cr alloy-treated oral mucosal models. **The human-derived full-thickness oral mucosal model was discriminatory between dental alloys and mechanistically provided insights into Ni-induced toxicity, highlighting potential clinical relevance.**

1 Introduction

Two-dimensional (2D) oral keratinocyte [1-**3**] and gingival fibroblast [**4-6**] cell monolayers have been employed to determine dental casting alloy biocompatibility. **Oral keratinocytes are the primary tissue target of nickel ions and have been associated with the proinflammatory response elicited by the oral mucosa during nickel hypersensitivity reactions *in vivo* [7]. However, the ability of cell monolayer structures to faithfully replicate the complexities of full-thickness human oral mucosal tissue have been questioned [7-9].** Cell monolayer structures possess deficiencies in cell differentiation [**10-11**], since anatomically cell monolayers fail to represent complex three-dimensional (3D) native human oral mucosal tissue. **Cell differentiation modifies a cell's ability to respond to chemical and hormonal signals due to changes in gene expression [12].** Additionally, cell monolayers lack supporting connective tissue, basement membranes and extracellular matrix [**13**] which can lead to increased toxin susceptibility and inappropriate immune responses.

Recent advances in tissue engineering have led to oral mucosal equivalent development with an *in vitro* translational advantage for biocompatibility testing [**8,13-15**]. Moharamzadeh et al. [**15**] incorporated primary gingival fibroblasts and immortalised TR146 oral keratinocytes onto a human-derived scaffold structure (Alloderm™) and identified cell differentiation, manifest as a cytokeratin expression profile similar to native human oral mucosal tissue, comprising cytokeratins 5, 10 and 19, indicative of cell type and epithelial differentiation status [**15**]. **However, the Moharamzadeh et al. [15] study could not be described as a primary cell-based structure as immortalised rather than primary oral keratinocytes were employed.**

Nickel-chromium (Ni-Cr) dental alloys were developed as a cost-effective alternative to Weinsteins high-gold patented alloy [**16**] in response to rising gold prices from 1968 [**17**]. **Co-Cr dental alloys possess similar elastic moduli, strength and hardness as Ni-Cr dental alloys, however, are less ductile compared with their Ni-Cr counterparts [18,19] and are accordingly not as widely employed in clinical dentistry.** Today Ni-Cr alloys are used extensively in fixed prosthodontics [**20-21**] where appliances can remain *in situ*, adjacent to the oral mucosa, for substantial periods of time and have been associated with nickel allergy - indicative of a type IV nickel-induced hypersensitivity response [**22**]. **Nickel allergy has been associated with dental appliances with metal-ceramic restorations manufactured using Ni-based dental casting alloys remaining in situ and directly adjacent to the oral mucosa for substantial periods of time [23-26]. Nickel is a potent allergen and carcinogen causing hypersensitivity reactions to a greater extent compared with any other metal used in metal-ceramic restorations with approximately one in five female and one in twenty male patients [27]. Consequently, the leaching of the metallic elemental components into the surrounding oral mucosal tissues should therefore be expected.**

The oral mucosal equivalent [**15**] was modified by replacing the immortalised cell line with primary oral keratinocytes, thereby creating an exclusively primary human cell-based tissue, termed the oral mucosal model, following integration into Alloderm™ scaffold structures. We hypothesised that the full-thickness oral mucosal model would provide an improved biocompatibility testing methodology for **base-metal** dental alloys and provide novel insights into the mechanisms of Ni-Cr alloy-induced toxicity. Assessment involved histological analyses in conjunction with analysis of

cell viability, oxidative stress responses, inflammatory cytokine expression and cellular toxicity.

2 Materials and Methods

2.1 Dental casting alloys

Ni-Cr (d.Sign®10 (in mass%: 75.4 Ni, 12.6 Cr and 8.0 Mo) and d.Sign®15 (58.7 Ni, 25.0 Cr and 12.1 Mo): Ivoclar Vivadent, Schaan, Liechtenstein) and Co-Cr (d.Sign®30 (30.1 Cr, 1.0 Mo and 60.2 Co): Ivoclar Vivadent) alloy-discs (10.0 mm diameter, 1.0 mm thickness) were cast, divested by alumina abrasion, polished to a clinical surface finish using rubber polishing wheels [2,28] and sterilised at 115°C for 15 min.

2.2 Cell culture

Prior ethical approval for the study was obtained from the Faculty of Ethical Research, Trinity College, Dublin, Ireland. All reagents were of cell culture grade supplied by Sigma-Aldrich Ltd. (Dublin, Ireland) or Invitrogen (Bio-Sciences Ltd., Dublin, Ireland). Buccal tissues, obtained on removing third molar teeth from informed healthy adults (n=15), were transferred to 10 mL 1x Dulbeccos' Phosphate Buffered solution (DPBS) and incubated (4°C) for 3 h. The tissue was washed with 10 mL Dulbeccos' Modified Eagle's Medium (DMEM) supplemented with 100 µg/mL penicillin, 100 µg/mL streptomycin and 2.5 µg/mL amphotericin B. The tissue was treated with 10 mL 2.5 mg/mL *Dispase I* in DMEM at 4°C for 12 h, prior to activation at 37°C for 30 min. The enzyme-treated tissue was transferred into 5 mL DMEM and connective tissue dissected from epithelial tissue.

The connective tissue was incubated in 10 mL 0.05% (w/v) collagenase type I at 37°C for 12 h, centrifuged (1500 rpm for 4 min) and re-suspended in 20 mL Green's Medium pH 7.0-7.4 (GM; 60% DMEM, 21% Hams F-12 Medium and supplemented

with 50 µg/mL penicillin, 50 µg/mL streptomycin, 10% foetal bovine serum (FBS), 2.5 µg/mL amphotericin B, 5 µg/mL insulin, 10 ng/mL human epidermal growth factor (EGF), $2x10^{-3}$ mol/L L-glutamine, 0.4 µg/mL hydrocortisone, 5 µg/mL transferring triiodothyronine and 10^{-4} mol/L adenine). Re-suspended connective tissue was inoculated into a T-25 cell culture flask (Cellcoat®, Greiner Bio-One Ltd., Gloucester, UK) and maintained under normal incubation conditions (5% CO_2 atmosphere at 37°C) with the GM media changed every 2-3 days.

The epithelial tissue was washed in 5 mL Keratinocyte Growth Medium (KGM; 64% DMEM, 23% Hams F-12 supplemented with 10% FBS, 100 µg/mL penicillin, 100 µg/mL streptomycin, 2.5 µg/mL amphotericin B, 10 ng/mL EGF, 0.5 µg/mL hydrocortisone, 5 µg/mL insulin, $1.8x10^{-4}$ M adenine and 10^{-10} M cholera toxin) followed by dissection. The tissue was re-suspended in 20 mL KGM, added to a T-25 cell culture flask and maintained under normal incubation conditions with the KGM media changed every 4-5 days.

At 70% confluence, the gingival fibroblast and oral keratinocyte cells were trypsinised using 10 mL 0.25% (w/v) trypsin-EDTA and incubated for 5 min. Detached cells were centrifuged (250*g* for 5 min), re-suspended in GM for gingival fibroblasts or KGM for oral keratinocytes. Cell densities required for seeding the oral mucosal model were established using the trypan blue dye assay [2].

Dehydrated Alloderm™ GBR (LifeCell Corp., Biohorizons UK, Berkshire, UK) discs (11.5 mm diameter, 4.6-4.8 mm thickness) were immersed in 10 mL 1x DPBS for 30 min and transferred into sterile 12.0 mm diameter polycarbonate inserts with a 0.4 µm

pore membrane (Corning® Transwell® insert, Fischer Scientific, Leicestershire, UK). The connective tissue aspect of the Alloderm™-disc was adjusted upwards and inoculated with gingival fibroblasts ($5x10^5$ cells in 800 µL GM). DMEM (800 µL) was added to the lower aspect and the structure incubated for 72 h.

The insert was re-opened and the Alloderm™ disc inverted so the connective tissue faced downwards. Oral keratinocytes ($5x10^5$ cells in 800µL KGM) were added to the basement membrane, the insert closed and re-incubated for 24 h. The GM and KGM were discarded, replaced with fresh media and incubated for a further 48 h. To encourage cell differentiation, the air/liquid interface was raised during incubation by reducing the 800 µL KGM to 250 µL over the next 4 days. **The sterilised alloy-discs were placed onto the basement membrane of the oral mucosal model and incubated submerged for the exposure-times specified for individual analyses.**

2.3 Histology

The oral mucosal models were embedded in OCT Tissue-Tek™ Containing Compound (Sakura Finetek, Syntec Scientific Ltd., Dublin, Ireland). The embedded oral mucosal models were incubated at -20ºC for 30 mins prior to cryosectioning to ensure the specimen matrix had frozen. Histological analyses of the untreated control and alloy-treated oral mucosal models were performed the cryo-sections (5 µm thickness) stained with haematoxylin and eosin (H&E) at 48 h.

Cryosectioning

Sections (5µm in thickness) were prepared using a hand-operated Cryostat (Leica CM1900, Leica Microsystems, Dublin, Ireland) which was maintained at a constant

temperature (-20 to -22ºC) and the sections were immediately placed onto subbed slides. The slides were incubated at room temperature for 5mins prior to staining with haematoxylin and eosin (H&E) to enhance the adhesion of the embedded oral mucosal model sections to the gelatine-based subbed slides.

2.4 Cell viability

The viability of the oral mucosal models following alloy-exposure were determined at 2, 24, 48 and 72 h (exposure-time) using the alamar blue resazurin salt assay, as a 10% solution in DMEM. Prior to the assay measurement, all test material was removed from the oral mucosal models, 500 µL of alamar blue dye added and incubated for 4 h. Aliquots (100 µL) were decanted into 96 well cell culture dishes and fluorescence intensity determined at excitation (530 nm) and emission (580 nm) wavelengths. Untreated oral mucosal models were the controls and all experiments performed in triplicate on three occasions.

2.5 Oxidative stress

Reduced glutathione (GSH) levels were determined for the untreated control and alloy-treated oral mucosal models using the GSH-Glo™ Glutathione assay (Promega, Dublin, Ireland) at 2, 24, 48 and 72 h (exposure-time). Untreated oral mucosal models were the controls and experiments performed in triplicate on three occasions.

2.6 Inflammatory cytokine expression

Inflammatory cytokine expression (Interleukin-1α (IL-1α), Interleukin-8 (IL-8), Prostaglandin E_2 (PGE_2) and Tumor Necrosis Factor-α (TNF-α)) from the oral mucosal models were assessed with ELISAs (Quantikine® Immunoassay Systems,

RnD Systems Ltd., Abingdon, UK) on 100 µL aliquots following alloy-exposure at 24 h. Untreated oral mucosal models were the controls and experiments performed in triplicate on three occasions.

2.7 LDH release

Cellular toxicity assessment of alloy-exposed oral mucosal models were determined by lactate dehydrogenase (LDH) release at 2, 24, 48 and 72 h (exposure time) using CytoTox 96® Non-Radioactive Cytotoxicity assays (Promega, Dublin, Ireland). Oral mucosal models treated with 1% Triton-X 100 (500 µL) were used as treated controls and experiments performed in triplicate on three occasions.

2.8 Inductively coupled plasma-mass spectrometry (ICP-MS)

Aseptic alloy-discs incubated in 50 mL DME for 1 day were diluted in deionised water 1:10 (pH 2.0) and analysed (Agilent 7500a Series® ICP-MS, Agilent Technologies, Dublin, Ireland). **Detection limits of ICP-MS analysis were in ng/L and cell culture media was used as a negative control for the ICP-MS analyses.**

2.9 Statistical Analyses

Linear regression analyses of the cell viability and cellular toxicity data for the controls and alloy-treated oral mucosal models with exposure time were used to determine cellular responses. One-way analysis of variance (ANOVA) and Tukey's post-hoc tests ($P<0.05$) were used for the pooled (all exposure times) cell viability, oxidative stress, inflammatory cytokine expression and cellular toxicity data for assessment of individual dental alloy (SPSS V12.0.1, SPSS Inc., IL, USA).

3 Results

3.1 Histological analyses

The Ni-Cr (d.Sign®10 and d.Sign®15) alloy-exposed oral mucosal models elicited critical losses of cellular thickness and compactness of epithelial and connective tissue layers (Figure 1b,c) compared with the untreated control oral mucosal model (Figure 1a). d.Sign®15 alloy-discs induced increased vacuolisation of connective tissue (Figure 1c) compared with d.Sign®10 (Figure 1b). No adverse morphological alterations were highlighted for the Co-Cr (d.Sign®30) alloy-discs (Figure 1d) compared with untreated control oral mucosal models (Figure 1a).

3.2 Cell viability

No significant metabolic decrease (P=0.5561) in the untreated control oral mucosal model was observed over 72 h and the positive regression slope suggested an active metabolic state (Table 1a, Figure 2a). Tukey's post-hoc tests showed significant decreases (P<0.0001) in cell viability following alloy-exposure compared with untreated control oral mucosal models. The d.Sign®15 alloy-discs elicited significantly decreased cell viability compared with d.Sign®10 (P<0.0001) and d.Sign®30 alloy-discs (P<0.0001). The d.Sign®10 alloy-discs elicited significantly decreased (P<0.0001) cell viability compared with d.Sign®30.

3.3 Oxidative stress

One-way ANOVA of the oxidative stress data for the alloy-treated oral mucosal models highlighted a significant decrease (P<0.0001) in reduced GSH compared with untreated control oral mucosal models. Tukey's post-hoc tests showed d.Sign®10 (P=0.0030) and d.Sign®15 (P<0.0001) alloy-discs elicited significant decreases in

reduced GSH but not d.Sign®30 (P=0.7280) alloy-discs when compared with untreated control oral mucosal models. The d.Sign®15 alloy-discs elicited significantly decreased reduced GSH from the oral mucosal models compared with d.Sign®10 (P=0.0230) and d.Sign®30 (P<0.0001) alloy-discs (Figure 2b).

3.4 Inflammatory cytokine expression

Inflammatory cytokine expression data from the alloy-exposed oral mucosal models highlighted significantly increased IL-1α (P<0.0190), IL-8 (P<0.0001), PGE_2 (P<0.0300) and TNF-α (P<0.0090) expression compared with untreated control oral mucosal models. The d.Sign®15 alloy-discs elicited significantly increased IL-1α (P<0.0001), IL-8 (P=0.0120), PGE_2 (P=0.0380) and TNF-α (P<0.0001) expression compared with d.Sign®10 alloy-discs. Ni-Cr alloy-discs significantly increased (P<0.0001) all inflammatory cytokine expression levels compared with Co-Cr alloy-discs (Figure 3a-d).

3.5 Cellular toxicity

Tukey's post-hoc tests on the pooled cellular toxicity data for alloy-exposed oral mucosal models showed the alloys elicited significantly increased LDH levels (P<0.0001) relative to the treated control oral mucosal models. The d.Sign®15 alloy-discs did not elicit significantly increased (P=0.5580) LDH levels compared with d.Sign®10 but did (P=0.0040) for d.Sign®30 alloy-discs. The LDH levels were not significantly increased (P=0.1130) for d.Sign®10 alloy-discs compared with d.Sign®30 alloy-discs (Figure 2c).

3.6 ICP-MS

The Ni-Cr alloy-discs (d.Sign®10 and d.Sign®15) leached high levels of nickel (<417.5 µg/L) and chromium (29.67 µg/L) ions, in addition to other alloying elements over the 14 day immersion duration. The Co-Cr alloy-disc (d.Sign®30) leached chromium (57.3 µg/L), iron (27.2 µg/L) and cobalt (17.3 µg/L), however, no nickel ions were detected.

4 Discussion

The current study produced a primary human cell-based oral mucosal model, integrated into Alloderm™ that permitted multiple-endpoint responses to dental alloy-discs. Alloderm™ is a low antigenic, durable [**29**], acellular human cadaveric dermis comprising a basal lamina suitable for keratinocyte attachment and growth and a lamina propria facilitating fibroblast infiltration and growth [**14**]. The oral mucosal model was viable as defined epithelial and connective tissue layers thickened, due to infiltration and growth of oral keratinocytes and gingival fibroblasts throughout the scaffold, with a defined boundary evident (Figure 1a). Therefore, the oral mucosal model was considered metabolically alive to a minimum of eleven days and histologically resembled native human oral mucosa. **Eleven days of culture was selected, as the oral mucosal model, was grown at the air-liquid interface for a total of 7 days and experimentation was performed on day 8 (2 hr), day 9 (24 h), day 10 (48 h) and day 11 (72 h).** The media employed in the oral mucosa model was serum-based in order to enhance the longevity of the primary cells employed compared with serum-free media [**30**]. We investigated the ability of the oral mucosal model to discriminate biocompatibility differences in **base-metal** dental alloy**s** and aimed to provide insight into the mechanisms of Ni-Cr alloy-induced toxicity.

Following Ni-Cr alloy-disc exposure, critical losses of cellular thickness and compactness of epithelial and connective tissue layers, vacuolisation of the connective tissue (d.Sign®10 (Figure 1b) and d.Sign®15 (Figure 1c)) and irreparable losses of tissue integrity were evident compared with the untreated control oral mucosal model and d.Sign®30 (Figure 1b) alloy-treated oral mucosal model (Figure 1a). The alamar blue dye assay for cell viability indicates barrier integrity in epithelial tissue [**31-32**].

The extensive loss of cell viability detected in the Ni-Cr alloy-treated oral mucosal models (Table 1a, Figure 2a) in conjunction with the histological data suggests nickel ions identified by ICP-MS (Table 1b) diffused throughout the epithelial tissue, to the basal lamina and subsequently throughout the extracellular matrix, resulting in loss of cell viability and tissue integrity. Generation of reactive oxygen species (ROS) by nickel ions and induction of oxidative stress are responsible for the rapid loss of cellular viability [1**,33**]. Low levels of ROS, present during normal cellular conditions are scavenged by major endogenous antioxidants (reduced glutathione (GSH)) [**34**]. Following Ni-Cr alloy-disc exposure, significant decreases ($P<0.0030$) in reduced GSH were evident (Figure 2b) compared with the untreated oral mucosal models and Co-Cr alloy-treated oral mucosal models, indicative of ROS generation, culminating in oxidative stress, loss of cellular viability and a potential immune response [**35**]. The increased nickel ion level in d.Sign®15 compared with the d.Sign®10 immersion solutions (Table 1b) were manifest as increased vacuolisation of the connective tissue and significantly decreased cell viability and significantly reduced GSH measurements.

Further evidence of lethal cell injury was provided by the LDH enzyme release assay, a marker of cell damage [**36-38**]. Triton-X treated oral mucosal models displayed high levels of LDH release at 2 h, indicative of maximum cellular toxicity, which was evident over 72 h and manifest as a negative regression slope (Table 1a, Figure 2c). Ni-Cr alloy-treated oral mucosal models elicited significantly increased LDH release ($P<0.0001$) with exposure-time and positive regression slopes, due to lysing of oral keratinocytes and gingival fibroblasts by nickel ions [**38**].

Activation of the innate immune response by nickel ions was indicated by the initiation of a proinflammatory response and recent data indicated that nickel ions activate innate immunity by stimulation of Toll-like receptor 4 (TLR4) proteins [**22**]. **Schmidt *et al*. [22] highlighted the link between the onset of nickel hypersensitivity in humans and the role of the surface membrane bound TLR4 proteins. During the secondary phase of nickel hypersensitivity *in vivo,* the proinflammatory response is elicited by the cells. The immune response elicited by the epithelial cells to nickel ions is thought to stimulate the production of TLR4-associated inflammatory cytokines IL-1α, IL-8, PGE_2 and TNF-α and other immune molecules including activated macrophages and phagocytes [39]. The initiation of the proinflammatory response by Ni^{2+} ions is thought to result from signals on membrane-bound receptors of which the TLR family are the most widely studied [22].** Mechanistically, the nickel ions are postulated to have permeated the epithelial tissue of the oral mucosal model and encountered surface membrane-bound TLR4 proteins [**22**] present on the surface of primary oral keratinocytes. Expression of IL-1α, IL-8, PGE_2 and TNF-α inflammatory cytokines may indicate the initiation of a type IV nickel-induced hypersensitivity response through TLR4 protein stimulation [**22**]. Low IL-1α, IL-8, PGE_2 and TNF-α expression were evident for the untreated oral mucosal models (Figure 3a-d) suggesting primary explant cells underwent stress, eliciting the immune responses observed. Following Ni-Cr alloy-disc exposure, significant IL-1α expression (Figure 3a) highlighted activation of epithelial inflammatory responses, indicative of cellular damage [**40**]. Significant IL-8 expression (Figure 3b) suggested the commencement of innate immunity responses [**2-3,41**] to the site of cellular injury [**41**] where elevated ROS occur [**35**]. Significant PGE_2 expression (Figure 3c), indicative of a chemically-

induced inflammatory response [**42**], signified the up-regulation of the epithelial inflammatory response [1], while significant TNF-α expression (Figure 3d) highlighted critical inflammatory levels - the end-point of the immune response [**35**].

The increased nickel ions leached from d.Sign®15 compared with d.Sign®10 immersion solutions (Table 1b) corroborated the inflammatory cytokine expression data, indicating that nickel release content was directly related to the level of immune response [**22**]. Consequently, d.Sign®15 alloy-treated oral mucosal models elicited significantly increased IL-1α [**40**], IL-8, [1**,41**], PGE_2 [**42**] and TNF-α [**43**] compared with d.Sign®10 alloy-treated oral mucosal models.

The authors acknowledge that it is difficult to completely replicate the *in vitro* conditions of the oral environment in an *in vivo* setting using oral mucosal models. However, the physical manifestation of nickel hypersensitivity reactions *in vivo* are well documented in the dental literature and the results obtained with the differentiated full-thickness oral mucosal models employed in the current study reflect the *in vivo* observations.

5 Conclusions

In summary, Ni-Cr alloy-exposure to the oral mucosal models resulted in vacuolisation of the connective tissue, loss of tissue integrity and a significant loss of cell viability with the initiation of a proinflammatory cytokine response and a significant reduction in reduced GSH levels, indicative of major oxidative damage. **It is proposed that nickel ions permeated the epithelial tissue of the oral mucosal model and interacted with TLR4 proteins, activating the proinflammatory responses observed with the rapid loss of cellular viability likely to have resulted from extreme oxidative damage.** Conversely, Co-Cr-treated oral mucosal models exhibited significantly improved biocompatibility compared with Ni-Cr-treated oral mucosal models. The Co-Cr-treated oral mucosal models had morphological appearance, reduced GSH levels, inflammatory cytokine expression and LDH release profiles similar to the untreated oral mucosal models since nickel was absent. The 3D human-derived, full-thickness, oral mucosal model described provides an improved biocompatibility testing methodology for discriminating between **base-metal** dental alloy and suggested novel insights into the mechanisms of Ni-Cr alloy-induced toxicity.

Acknowledgements

The authors would like to thank Dr Keyvan Moharamzadeh and Professor Richard van Noort, School of Clinical Dentistry, University of Sheffield, UK for training on their oral mucosal equivalent and Dublin Dental University Hospital for the provision of funding for this project.

References

1. Trombetta D, Mondello MR, Cimino F, Cristani M, Pergolizzi S, Saija A. Toxic effects of nickel in an in vitro model of human oral epithelium. Toxicol Lett 2005;159:219-225.
2. McGinley EL, Coleman DC, Moran GP, Fleming GJP. Effects of surface finishing condition on the biocompatibility of a nickel-chromium dental casting alloy. Dent Mater 2011;27:637-650.
3. **Wylie CM, Davenport AJ, Cooper PR, Shelton RM. Oral keratinocyte responses to nickel-based dental casting alloys in vitro. J Biomater Appl 2010;25:251-267.**
4. Messer RL, Bishop S, Lucas LC. Effects of metallic ion toxicity on human gingival fibroblasts morphology. Biomaterials 1999;20:1647-1657.
5. Issa Y, Brunton P, Waters CM, Watts DC. Cytotoxicity of metal ions to human oligodendroglial cells and human gingival fibroblasts assessed by mitochondrial dehydrogenase activity. Dent Mater 2008;24:281-287.
6. Elshahawy W, Watanabe I, Koike M. Elemental ion release from four different fixed prosthodontic materials. Dent Mater 2009;25:976-981.
7. Chai WL, Moharamzadeh K, Brook IM, Emanuelsson L, Palmquist A, van Noort R. Development of a novel model for the investigation of implant-soft tissue interface. J Periodontol 2010:81;1187-1195.
8. Moharamzadeh K, Brook IM, Scutt AM, Thornhill MH, Van Noort R. Mucotoxicity of dental composite resins on a tissue-engineered human oral mucosal model. J Dent 2008a;36:331-336.

9. Kinikoglu B, Auxenfans C, Pierrillas P, Justin V, Breton P, Burillon C et al. Reconstruction of a full-thickness collagen-based human oral mucosal equivalent. Biomaterials 2009;30:6418-6425.

10. Moharamzadeh K, Franklin KL, Brook IM, van Noort R. Biologic assessment of antiseptic mouthwashes using a three-dimensional human oral mucosal model. J Periodontol 2009;80:769-775.

11. Moharamzadeh K, Brook IM, Van Noort R, Scutt AM, Thornhill MH. Tissue-engineered oral mucosa: a review of the scientific literature. J Dent Res 2007;86:115-124.

12. Allombert-Blaise C, Tamiji S, Mortier L, Fauvel H, Delaporte E, Piette F, Martin DeLassale E, et al. Terminal differentiation of human epidermal keratinocytes involves mitochondria and caspase dependant cell death pathway. Cell Death Differ 2003;10:850-852.

13. Klausner M, Ayehunie S, Breyfogle BA, Wertz PW, Bacca L, Kubilus J.Organotypic human oral tissue models for toxicological studies. Toxicol In Vitro 2007;21:938-949.

14. Izumi K, Terashi H, Marcelo GL, Feinberg SE. Development and characterization of a tissue-engineered human oral mucosal equivalent produced in a serum-free culture system. J Dent Res 2000;79:798-805.

15. Moharamzadeh K, Brook IM, Van Noort R, Scutt AM, Smith KG, Thornhill MH. Development, optimization and characterization of a full-thickness tissue engineered human oral mucosal model for biological assessment of dental biomaterials. J Mater Sci: Mater Med 2008b;19:1793-1801.

16. Weinstein M, Katz S, Weinstein AB. Permanent Manufacturing Corporation, Assignee: fused porcelain-to-metal teeth. US Patent No. 3052982, 1962.

17. Tuccillo JT, Cascone PJ. The evolution of porcelain-fused-to-metal (PFM) alloy systems. In: McLean JW, editor. Dental ceramics: Proceedings of the first international symposium on ceramics. IL, USA: Quintessence Publishing; 1983.

18. Roach MR. Base metal alloys used for dental restorations and implants. Dent Clin North Am 2007;51:603-627.

19. Reclaru L, Lüthy H, Eschler PY, Blatter A, Susz C. Corrosion behaviour of cobalt-chromium dental alloys doped with precious metals. Biomaterials 2005;26:4358-4365.

20. Morris HF. Veteran's administration co-operative studies project no 147. part IV: biocompatibility of base metal alloys. J Prosthet Dent 1987;58:1-5.

21. Rosentiel SF, Land MF, Fujimoto J. Contemporary fixed prosthodontics. Edinburgh: Elsevier Mosby Saunders; 2006.

22. Schmidt M, Raghavan B, Müller V, Vogl T, Fejer G, Tchaptchet S, Keck S, et al. Crucial role for human Toll-like receptor 4 in the development of contact allergy to nickel. Nat Immunol 2010;11:814-819.

23. Fors R, Persson M. Nickel in dental plaque and saliva in patients with and without orthodontic appliances. Eur J Orthod 2006;28:292-297.

24. Counts AL, Miller MA, Khakhria ML, Strange S. Nickel allergy associated with a transpalatal arch appliance. J Orofac Orthoped 2002;63:509-515.

25. Jia W, Beatty MW, Reinhardt RA, Petro TM, Cohen DM, Maze CR, Strom EA et al. Nickel release from orthodontic arch wires and cellular immune response to various nickel concentrations. J Biomed Mater Res: App Biomater 1999;48:488-495.

26. Bumgardner JD, Lucas LC. Cellular response to metallic ions released from nickel-chromium dental alloys. J Dent Res 1995;74:1521-1527.

27. Noble J, Ahing SI, Karaiskos NE, Wiltshire WA. Nickel allergy and orthodontics, a review and report of two cases. Brit Dent J 2008;204:297-300.

28. Wylie CM, Shelton RM, Fleming GJP, Davenport AJ. Corrosion of nickel-based dental casting alloys. Dent Mater 2007;23:714-723.

29. Ghosh MM, Boyce S, Layton C, Freelander E, MacNeil S. A comparison of methodologies for the preparation of human epidermal-dermal composites. Ann Plas Surg 1997;39:390-404.

30. Grafström RC. Human oral epithelium. In: Freshney RI, Freshney MG, editors. Culture of epithelial cells. Wiley-Liss; 2002. p.196-254.

31. Nakayama GR, Caton MC, Nova MP, Parandoosh Z. Assessment of the alamar blue assay for cellular growth and viability in vitro. J Immunol Methods 1997;26:205-208.

32. Gloeckner H, Jonuleit T, Lemke HD. Monitoring of cell viability and cell growth in a hollow fiber bioreactor by use of the dye alamar blue. J Immuno Mater 2001;252:131-138.

33. Maiese K, Chong ZZ, Hou J, Shang YC. Oxidative stress: biomarkers and novel therapeutic pathways. Exp Gerontol 2010;45:217-234.

34. Chong ZZ, Li F, Maiese K. Oxidative stress in the brain: novel cellular targets that govern survival during neurodegenerative disease. Prog Neurobio 2005;75:207-246.

35. Vlahopoulos S, Boldogh I, Casola A, Brasier AR. NF-$_K$B-dependant induction of interleukin-8 gene expression by tumor necrosis factor alpha: evidence for an antioxidant sensitive activating pathway distinct from nuclear translocation. Blood 1999;94:1878-1889.

36. Lash LH, Tokarz JJ, Pegouske DM. Susceptibility of primary cultures of proximal tubular and distal tubular cells from rat kidney to chemically induced toxicity. Toxicology 1995;103:85-103.

37. Issa Y, Watts DC, Waters CM, Duxbury AJ. Resin composite monomers alter MTT and LDH activity of human gingival fibroblasts in vitro. Dent Mater 2004;20:12-20.

38. Kendig DM, Tarloff JB. Inactivation of lactate dehydrogenase by several chemicals: implications for in vitro toxicology studies. Toxicol In Vitro 2007;21:125-132.

39. Grabbe S, Schwarz T. Immunoregulatory mechanisms involved in elicitation of allergic contact dermatitis. Immuno Today 1998;19:37-44.

40. Curtis A, Morton J, Balafa C, MacNeil S, Gawkrodger DJ, Warren ND, Evans GS. The effects of nickel and chromium on human keratinocytes: differences in viability, cell associated metal and IL-1α release. J Toxicol 2007;21:809-819.

41. Schmalz G, Schweikl H, Hiller KA. Release of prostaglandin E_2, IL-6 and IL-8 from human oral epithelial culture models after exposure to compounds of dental materials. Eur J Oral Sci 2000;108:442-448.

42. Dongari-Bagtzoglou AI, Ebersole JL. Production of inflammatory mediators and cytokines by human gingival fibroblasts following bacterial challenge. J Periodontal Res 1996;31:90-98.

43. Vermeulen K, Bockstaele DR, Berneman ZN. Apoptosis: mechanisms and relevance in cancer. Ann Hematol 2005;84:627-639.

Figure Captions

Figure 1: Histological assessment (following 11 day incubation) of (a) the untreated control oral mucosal model and the alloy-treated oral mucosal models following exposure to (b) d.Sign®10, (c) d.Sign®15 and (d) d.Sign®30 alloy-discs.

Figure 2: Graphical representation (with standard error bars) of the (a) cell viability, (b) oxidative stress response and (c) cellular toxicity analyses of the control oral mucosal models and the alloy-treated oral mucosal models following 2-72 h exposure to the d.Sign®10, d.Sign®15 and d.Sign®30 discs.

Figure 3: Boxplot analysis (with standard error bars) of (a) IL-1α, (b) IL-8, (c) PGE_2 and (d) TNF-α inflammatory cytokine expression (in pg/mL) from the untreated control oral mucosal models and the alloy-treated oral mucosal models following 24 h exposure to the d.Sign®10, d.Sign®15 and d.Sign®30 alloy-discs.

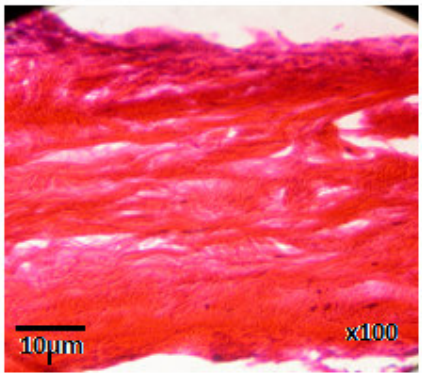

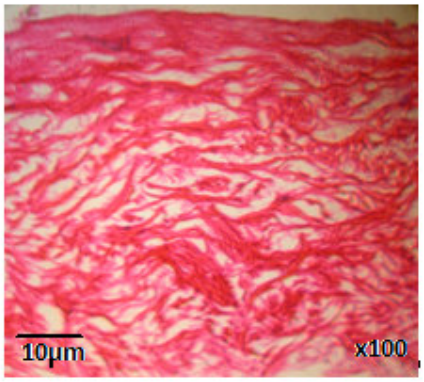

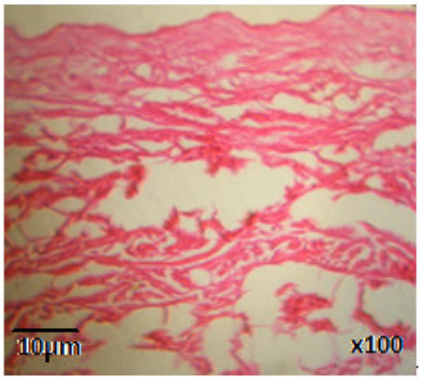

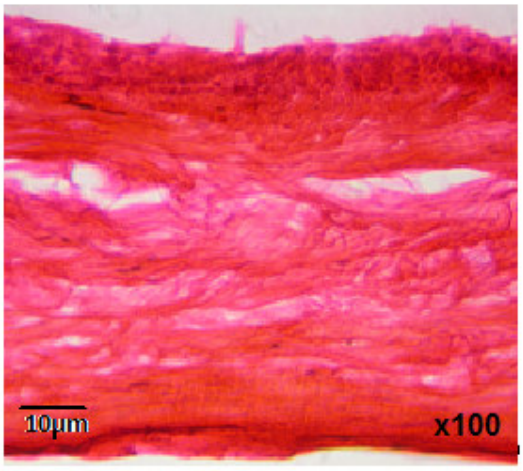

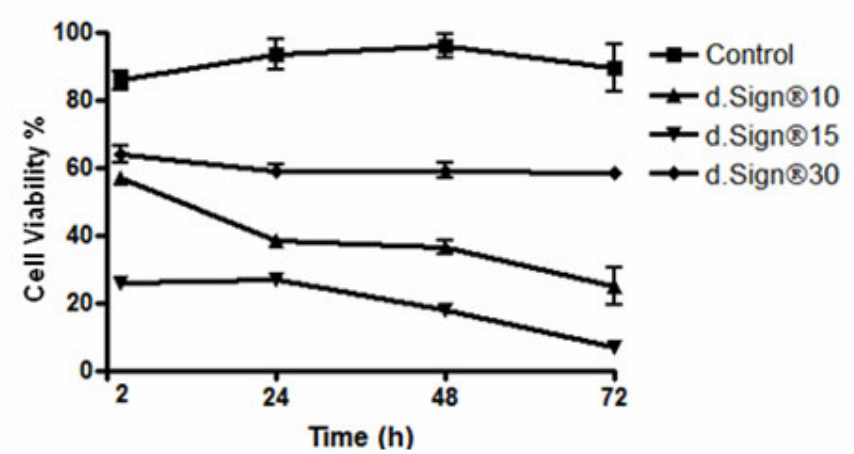

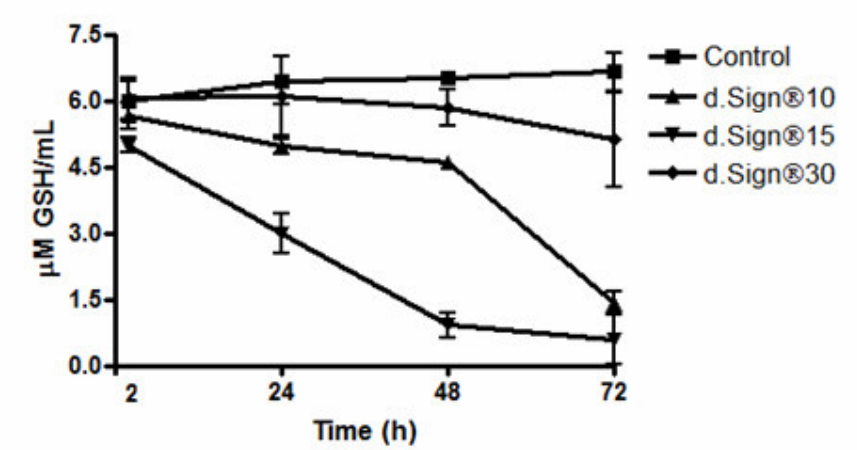

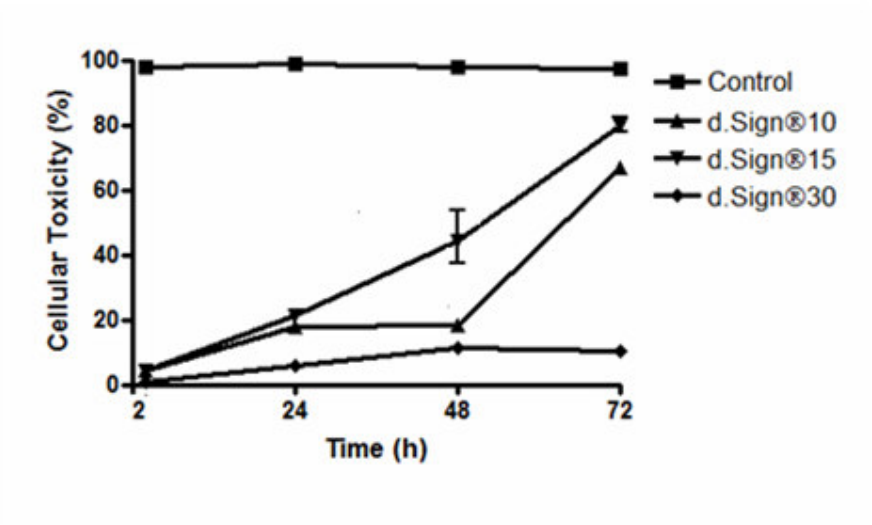

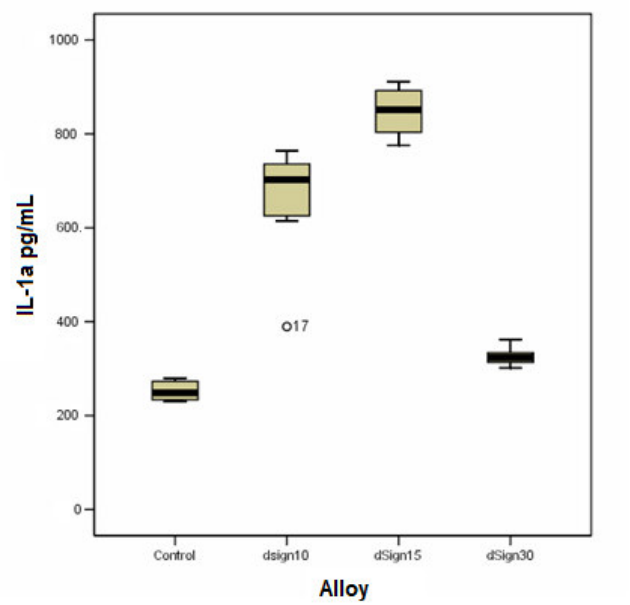

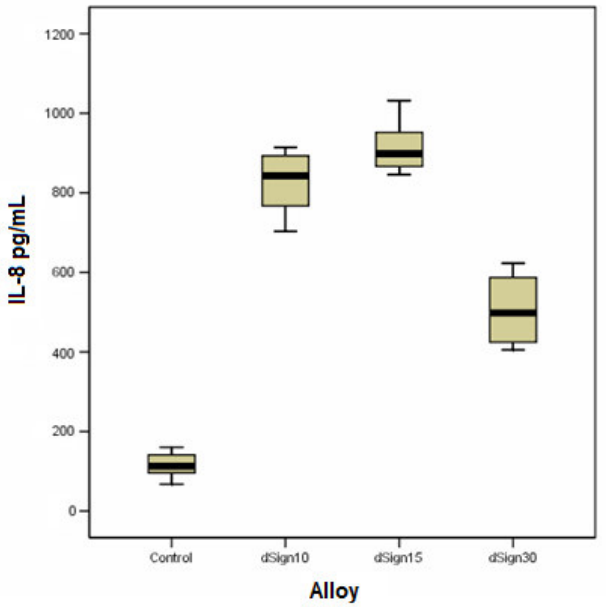

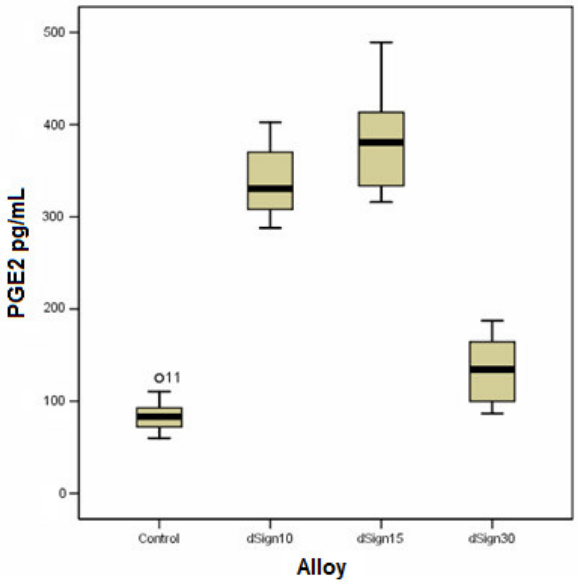

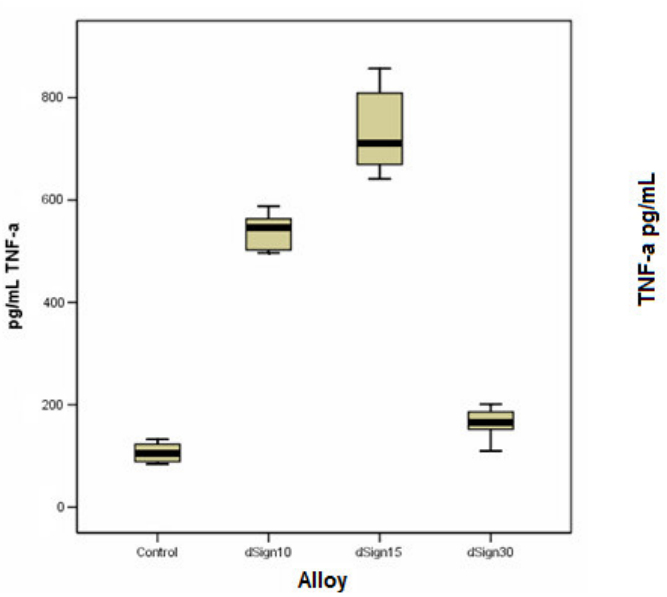

Table 1a: Linear regression analysis data for the cell viability and cellular toxicity data for exposure time (2-72 h) - the control oral-mucosal-model and alloy-exposed oral-mucosal-models. (equation of the line: $y = mx + c$ where m=slope and c=intercept with y-axis, r^2: coefficient of determination, P value: probability and df: degrees of freedom).

Cellular Assay	Alloy	Equation of the Line	r^2	P value	df
Cell Viability	**Control**	y=1.3x + 87.8	0.0357	0.5561	10
	d.Sign®10	y=-9.8x + 63.7	0.7912	0.0001	10
	d.Sign®15	y=-6.6x + 35.9	0.8006	0.0001	10
	d.Sign®30	y=-1.6x + 64.0	0.2496	0.0981	10
Cellular Toxicity	**Control**	y=-0.3x + 98.7	0.6555	0.4218	10
	d.Sign®10	y=18.4x – 19.5	0.7932	0.0001	10
	d.Sign®15	y=24.9x – 24.8	0.7680	0.0002	10
	d.Sign®30	y=3.4x – 1.5	0.7651	0.0002	10

Table 1b: ICP-MS analysis of the 1 day immersion solutions for the d.Sign®10, d.Sign®15 and d.Sign®30 alloy-discs. Values are given in µg/L.

Alloy	Day	Ni	Cr	Mo	Fe	Co	Cu
d.Sign®10	**1**	68.4	11.5	17.4	52.4	-	240.7
d.Sign®15	**1**	140.8	14.5	25.4	67.1	-	267.1
d.Sign®30	**1**	-	37.4	-	12.8	25.1	-